

A Comprehensive Expressed Sequence Tag Linkage Map for Tiger Salamander and Mexican Axolotl: Enabling Gene Mapping and Comparative Genomics in *Ambystoma*

J. J. Smith,^{*,1} D. K. Kump,^{*} J. A. Walker,^{*} D. M. Parichy[†] and S. R. Voss^{*}

^{*}Department of Biology, University of Kentucky, Lexington, Kentucky 40506 and [†]Section of Integrative Biology, Section of Molecular, Cell and Developmental Biology, Institute for Cellular and Molecular Biology, University of Texas, Austin, Texas 78705

Manuscript received June 8, 2005
Accepted for publication July 26, 2005

ABSTRACT

Expressed sequence tag (EST) markers were developed for *Ambystoma tigrinum tigrinum* (Eastern tiger salamander) and for *A. mexicanum* (Mexican axolotl) to generate the first comprehensive linkage map for these model amphibians. We identified 14 large linkage groups (125.5–836.7 cM) that presumably correspond to the 14 haploid chromosomes in the *Ambystoma* genome. The extent of genome coverage for these linkage groups is apparently high because the total map size (5251 cM) falls within the range of theoretical estimates and is consistent with independent empirical estimates. Unlike most vertebrate species, linkage map size in *Ambystoma* is not strongly correlated with chromosome arm number. Presumably, the large physical genome size (~30 Gbp) is a major determinant of map size in *Ambystoma*. To demonstrate the utility of this resource, we mapped the position of two historically significant *A. mexicanum* mutants, *white* and *melanoid*, and also *met*, a quantitative trait locus (QTL) that contributes to variation in metamorphic timing. This new collection of EST-based PCR markers will better enable the *Ambystoma* system by facilitating development of new molecular probes, and the linkage map will allow comparative studies of this important vertebrate group.

THE tiger salamander (*Ambystoma tigrinum*) species complex consists of several closely related and phenotypically diverse taxa that range from central Mexico to southern Canada (SHAFFER and MCKNIGHT 1996). The complex as a whole is an important, naturalistic model system because taxa are characterized by extensive interspecific and intraspecific variation for a number of ecologically important traits, including expression of metamorphic *vs.* nonmetamorphic (paedomorphic) life histories (GOULD 1977; SHAFFER and VOSS 1996), timing of metamorphosis (ROSE and ARMENTROUT 1976; VOSS and SMITH 2005), cannibal *vs.* normal larval morphologies (POWERS 1907; HOFFMAN and PFENNIG 1999), infectious disease (COLLINS *et al.* 2004), variation in adult coloration and pigment patterning (REESE 1969; PARICHY 1996, 1998), and variation in general morphology (SHAFFER 1984; IRSCHICK and SHAFFER 1997). In addition, these salamanders are important laboratory models for olfaction (MARCHAND *et al.* 2004; PARK *et al.* 2004), vision (THORESON *et al.* 2004; CHICHILNISKY and REIKE 2005), cardiogenesis (DENZ *et al.* 2004; ZHANG *et al.* 2004), embryogenesis (BACHVAROVA *et al.* 2004; ERICSSON *et al.* 2004), and postembryonic development (PARICHY 1998; VOSS and SMITH 2005), including organ and tissue

regeneration (CHRISTENSEN *et al.* 2002; SCHNAPP and TANAKA 2005). Both natural and laboratory-based research areas are in need of a comprehensive genome map that can be used to identify the position and effect of loci that contribute to phenotypic variation and that can be used to compare features of the salamander genome to other vertebrates. Moreover, molecular markers that are used to develop linkage maps provide the material for generating nucleotide probes and sequences that can be used in a variety of ways, including *in situ* hybridization, population genetics, systematics, molecular evolution, and functional genomics.

Several lines of evidence suggest that meiotic or recombinational map size is large in tiger salamanders. The earliest mapping studies in *A. mexicanum* employed tetrad analysis and gynogenic salamanders for estimating genetic distance between a few phenotypic markers and their centromeres (*e.g.*, three in LINDSLEY *et al.* 1955 and seven in ARMSTRONG 1984). Most of these phenotypes were mapped to positions distant from centromeres (unlinked); this suggests a large recombinational map size for *Ambystoma* relative to other vertebrates where the majority of loci typically show linkage with the centromere (BROWN *et al.* 1998; STEEN *et al.* 1999; GROENEN *et al.* 2000; KELLY *et al.* 2000; KONG *et al.* 2002). Using a more direct method, CALLAN (1966) reported chiasmata counts from *A. mexicanum* oocyte nuclei ranging from 101 to 126, averaging 113 chiasmata per

¹Corresponding author: Department of Biology, University of Kentucky, Lexington, KY 40506. E-mail: jjsmit3@uky.edu

TABLE 1
Relationships between genome size and map size in vertebrates

Organism	Genome size (Gbp) ^a	<i>N</i> ^b	Chromosomal arms ^b	Map size (cM) ^c	Obligatory map (<i>N</i> × 50 cM)	Proportion obligatory ^d	cM/arm
Mouse	2.7	20	20	1361	1000	0.73 (0.73)	68.1
Rat	2.6	21	33	1749	1050	0.60 (0.94)	53.0
Human	3.0	23	46	3615	1150	0.32 (0.64)	78.6
Chicken	1.2	38	44	3800	1900	0.50 (0.58)	86.4
Zebrafish	1.8	25	50	3011	1250	0.42 (0.83)	60.2
Ambystoma (map) ^e	30.0	14	28	5152	700	0.14 (0.27)	184.0
Ambystoma (χ) ^f	30.0	14	28	5650	700	0.12 (0.25)	201.8

^aReferences: mouse, MOUSE GENOME SEQUENCING CONSORTIUM (2002); rat, RAT GENOME SEQUENCING PROJECT CONSORTIUM (2004); human, INTERNATIONAL HUMAN GENOME SEQUENCING CONSORTIUM (2000); chicken, INTERNATIONAL CHICKEN GENOME SEQUENCING CONSORTIUM (2005); zebrafish, KELLY *et al.* (2000); Ambystoma, LICHT and LOWCOCK (1991).

^bThe haploid number of chromosomes. Smaller chicken microchromosomes (10–38; MASABANDA *et al.* 2004) are tabulated as one-armed chromosomes. References: mouse, MOUSE GENOME SEQUENCING CONSORTIUM (2002); rat, RAT GENOME SEQUENCING PROJECT CONSORTIUM (2004); human, INTERNATIONAL HUMAN GENOME SEQUENCING CONSORTIUM (2000); chicken, INTERNATIONAL CHICKEN GENOME SEQUENCING CONSORTIUM (2005); zebrafish, GORNUNG *et al.* (2000); Ambystoma, CALLAN (1966).

^cReferences: mouse, Steen *et al.* (1999); rat, BROWN *et al.* (1998); human, KONG *et al.* (2002); chicken, GROENEN *et al.* (2000); zebrafish, KELLY *et al.* (2000).

^dNumbers in parentheses represent the obligatory proportion of the map assuming one obligate chiasma per arm.

^eMap size is estimated as the sum of LG1–14.

^fMap size is estimated as 50 cM × the average number of chiasmata (CALLAN 1966).

nucleus. Assuming that one crossover is equivalent to a 50-cM map distance (STURTEVANT 1913), this chiasmata frequency converts to an estimated map distance of 5650 cM, which is ~4.2× larger than that of the mouse genome and 1.6× larger than that of the human genome (Table 1). Finally, Voss *et al.* (2001) estimated map size from a linkage analysis in which 347 molecular genotypes were obtained for offspring from backcrosses between *A. mexicanum* and *A. mexicanum/A. t. tigrinum* hybrids. That analysis yielded one of the largest partial genetic linkage maps ever constructed (~3400 cM) and an overall map size estimate of 7291 cM based on the method of HULBERT *et al.* (1988). Thus, all studies to date suggest that recombinational map size is relatively larger in Ambystoma than in other vertebrates. Although recombinational map size in Ambystoma may simply be a consequence of a large physical genome size (Table 1), the contribution of additional factors that are known to strongly influence map length in other vertebrates (*e.g.*, chromosome number and morphology) have not been considered.

Recently completed expressed sequence tag (EST) sequencing projects for two tiger salamander species, *A. mexicanum* (HABERMAN *et al.* 2004; PUTTA *et al.* 2004) and *A. tigrinum tigrinum* (PUTTA *et al.* 2004), allowed us to rapidly develop a sufficient number of EST-based markers to generate a comprehensive genetic map for Ambystoma, and the first such map for any amphibian. Below we describe this new resource and show its utility in two areas: (1) mapping phenotypic mutants and (2) investigating the relative effects of genome size and chromosome number on recombination-based estimates of genome size. We also note the importance of these EST-

based PCR markers as a general resource for tiger salamander research.

MATERIALS AND METHODS

Study species: *A. tigrinum tigrinum*: The Eastern tiger salamander is the archetype of the tiger salamander species complex. This relatively large salamander species breeds in ponds and temporary pools in the eastern and southern parts of the United States; the individual that was used in this study was purchased from Charles D. Sullivan, which collects and distributes amphibians from breeding ponds in the vicinity of Nashville, Tennessee. These salamanders undergo a typical amphibian life cycle, wherein they hatch from the egg in an aquatic-larval form and eventually undergo a metamorphosis through which they achieve a terrestrial adult form.

A. mexicanum: The Mexican axolotl is native to a single lake in central Mexico (Lake Xochimilco, Mexico D.F., Mexico). It is commonly used in biological research and strains have been maintained in laboratory culture for nearly a century and a half (DUMERIL 1870; see also review by SMITH 1989). The most notable feature of this salamander is that it exhibits a phenotype, known as paedomorphosis, wherein it forgoes metamorphic changes typical of most ambystomatid salamanders and retains a largely larval morphology throughout adult life. Several developmental mutants have been described for *A. mexicanum* (MALACINSKI 1989) and are readily available (<http://www.ambystoma.org>). We estimated the genomic position of two recessive pigment mutants: *white* (HÄCKER 1907) and *melanoid* (HUMPHREY and BAGNARA 1967). In comparison to wild type, *white* is characterized by a general lack of epidermal pigment cells, which is caused by failure of pigment cell precursors to migrate or survive in epidermal tissues (reviewed by PARICHY *et al.* 1999). In comparison to wild type, *melanoid* is characterized by a lack of iridophores in the skin and iris, relatively fewer xanthophores and greater numbers of melanophores (HUMPHREY and BAGNARA 1967).

Molecular markers: A total of 1095 molecular markers were genotyped using a previously described AxTg mapping family that was generated by backcrossing *A. mexicanum*/*A. t. tigrinum* F₁ hybrids to a single *A. mexicanum* (Voss 1995). In a previous study using AxTg, Voss *et al.* (2001) reported linkage analyses of 323 “anonymous” molecular markers (315 AFLPs and 8 RAPDs) and 24 markers for nuclear protein-coding sequences. Here we report an additional 202 AFLP markers (scored for 44 backcross offspring) and 546 EST-based markers (scored for 91 backcross offspring). Marker fragments were amplified using standard PCR conditions (150 ng DNA, 50 ng each primer, 1.2 mM MgCl₂, 0.3 units Taq polymerase, 1× PCR buffer, 200 mM each of dATP, dCTP, dGTP, dTTP; thermal cycling at 94° for 4 min; 33 cycles of 94° for 45 sec, 60° for 45 sec, 72° for 30 sec; and 72° for 7 min). Polymorphisms were diagnosed by primer extension [Perkin-Elmer (Norwalk, CT) AcycloPrime-FP chemistry and Wallac (Gaithersburg, MD) Victor3 plate reader] (*e.g.*, CHEN *et al.* 1999; HSU *et al.* 2001; GARDINER and JACK 2002), thermal-gradient capillary gel electrophoresis (SpectruMedix, Reveal), allele-specific amplification, PCR fragment size polymorphism, and restriction digestion. Primer sequences, diagnostic polymorphisms, polymorphism detection assays, numbers of individuals genotyped, and NCBI GI numbers for source sequences for all 570 protein-coding loci are summarized in supplementary Table S1 at <http://www.genetics.org/supplemental/>. The design of AFLP markers, EST-based markers, and primer extension probes is described in detail below.

Generation of AFLP and RAPD markers: The methods used to generate AFLPs and RAPDs were reported previously (VOSS and SHAFFER 1997; VOSS *et al.* 2001). An additional 202 AFLPs were generated for this study using the same methods and backcross progeny. Primer sequences for all AFLPs are provided in supplementary Table S2 at <http://www.genetics.org/supplemental/>.

EST-based marker design: The majority of EST-based markers were designed to target 3′-unconserved regions of assembled EST sequences that were derived from *A. mexicanum* and *A. t. tigrinum* (PUTTA *et al.* 2004). These sequences were identified by first aligning (BLASTx) assembled sequences to a custom database of human protein sequences (Ref Seq Release 3, NCBI). The 3′-most 70 bp of aligning sequence and all remaining nonaligning 3′ sequence were targeted for primer design. These regions presumably correspond to sequence encoding carboxy-terminal regions and 3′-untranslated regions. Primers were designed within these regions using Primer3 software (<http://www.mit.wi.edu/Primer3.html>). When presumably orthologous sequences (>90% identity) were available for both *A. mexicanum* and *A. t. tigrinum*, marker design was additionally constrained to flank at least one polymorphism between the two sequences.

Primer extension probe design: Primer extension probes were designed to target polymorphisms that were observed between presumptively orthologous EST sequences or between EST sequences and sequenced marker fragments that were amplified from *A. mexicanum* and *A. t. tigrinum*. Design of primer extension probes was constrained such that probes were complementary to sequence immediately 3′ of targeted SNP positions. The software package Array Designer 2.1 (PREMIER Biosoft International) was used to identify probes with T_m 60° ± 8° and high Δ*g* for primer hairpin and primer dimer formation.

Construction of the linkage map: A linkage map was constructed for the tiger salamander using genotypes for 570 protein-coding markers (EST and gene based) and 525 AFLP markers. Linkage analyses were performed using Mapmaker/EXP 3.0b and linkage groups (LG) were visualized using MapManagerQXTb19 (MEER *et al.* 2004) and MapChart 2.1

(VOORIPS 2002). This linkage map was constructed by first identifying sets of markers that formed linear linkage groups supported by a log of odds (LOD) ≥5.0 and then by recursively adding markers to these initial groups at lower LOD thresholds (4.0, 3.5, and 3.0). At each step linkage groups were visually inspected to verify the linear arrangement among markers. At each LOD threshold, the addition of new markers to an existing linkage group or merger of two existing linkage groups was constrained such that addition or merger did not disrupt arrangements that were previously set at a higher LOD threshold. A few markers could not be assigned to precise positions within a linkage group, but could be assigned to a single linkage group at LOD >4.0 (supplementary Table S2 at <http://www.genetics.org/supplemental/>). Linkage distances among markers in the final map were estimated using the KOSAMBI (1944) mapping function in MapManagerQXTb19 (MEER *et al.* 2004).

QTL analysis: Interval analysis was used to identify the positions of two mutant phenotypes that segregated within the AxTg mapping family: *white*, which is specified by the recessive locus *d*, and *melanoid*, which is specified by the recessive locus *m*. Interval analysis was also used to identify the position of a major-effect QTL that contributes to segregation of metamorphosis *vs.* paedomorphosis and developmental timing. Segregation patterns of *white*, *melanoid*, and metamorphic phenotypes within the AxTg family have been previously described (Voss 1995). Likelihood-ratio statistics (LRS) for association of phenotypic variation with genotypic inheritance were estimated using the interval mapping (*e.g.*, HALEY and KNOTT 1992; MARTINEZ and CURNOW 1992; ZENG 1993, 1994) function of MapManagerQTXb19 (MEER *et al.* 2004). Significance thresholds for interval mapping were obtained through 10,000 permutations of trait values among backcross progeny. Confidence intervals for QTL positions were estimated by the method of DARVASI and SOLLER (1997).

RESULTS

Segregation of molecular markers: The segregation of alternate genotypes for a majority of the molecular markers was consistent with the Mendelian expectation of 1:1. Only 7% of protein-coding markers had genotypic ratios exceeding the 95% tail of the χ^2 distribution (Figure 1A). On average, ratios of anonymous markers were more deviant than those of protein-coding markers with 17% of markers exceeding the 95% tail of the χ^2 distribution (Figure 1B). Plotting χ^2 values for both marker classes against genomic position showed that the few markers with significantly deviant ratios were not strongly clustered at any position within the genome (Figure 1C).

Linkage analysis: Linkage analysis revealed 14 large linkage groups that ranged in size from 125.5 to 836.7 cM and consisted of 14–123 markers (Figure 2, Table 2). A total of 790 markers were assigned to these 14 linkage groups, with 486 protein-coding loci and 169 anonymous loci placed at precise positions. The total linkage distance spanned by these markers was 5251.3 cM and the average intermarker distance was 7.96 cM.

Thirty-six smaller linkage groups that ranged in size from 0 to 79 cM and consisted of 2–10 markers were identified. Thirteen of these linkage groups contained

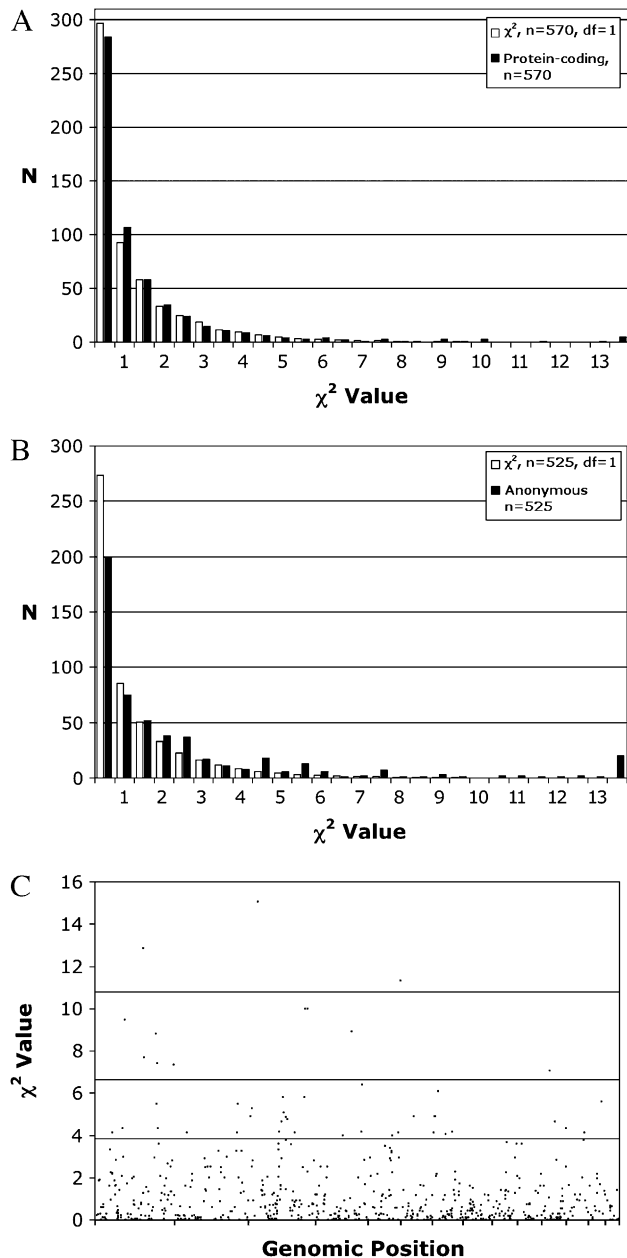


FIGURE 1.—(A) Plot of the distribution of the χ^2 statistic for 1:1 segregation of marker genotypes *vs.* standard χ^2 distributions for gene and EST-based markers. (B) Plot of the distribution of the χ^2 statistic for 1:1 segregation of marker genotypes *vs.* standard χ^2 distributions for anonymous markers (AFLPs and RAPDs). (C) Plot of χ^2 statistics for 1:1 segregation of marker genotypes *vs.* map position. The *x*-axis represents LG1–14 concatenated head to tail, and vertical bars demark boundaries between linkage groups.

at least one EST or protein-coding marker and spanned a total of 479.7 cM; 23 additional linkage groups that consisted of only AFLP markers spanned a total of 630.5 cM. A total of 165 markers (134 AFLP and 31 protein coding) did not show linkage to any other marker and were not assigned to any of the linkage groups.

QTL analyses: *white*: Interval analysis identified two LRS peaks for *white* on LG1 (*D1*, LRS 37.2, 95% C.I. =

17 cM; *D2*, LRS 12.4, 95% C.I. = 44 cM) (Figure 3). Although this suggests the possibility that *white* may depend upon more than a single locus, the lesser LRS peak is only suggestive of a significant QTL and an equally supportive LRS is expected to be observed once at random within the genome. In the mapping cross, color phenotypes segregated as F_2 -type markers because F_1 hybrids and the recurrent *A. mexicanum* carried a single recessive allele (*d*) at *white* (D^{sig}/d^{mex} and D^{mex}/d^{mex} genotypes, respectively). In contrast, molecular genotypes segregated as backcross-type markers. As a result, only the *A. tigrinum* marker alleles were fully informative for association testing; that is, we expected that at the position of *white*, all individuals inheriting *A. tigrinum* molecular marker alleles would exhibit wild-type coloration, but never *white* coloration. Segregation ratios for two protein-coding markers (*E16A12* and *E23C5*) near the maximum LRS peak on LG1 are consistent with this expectation (Table 3). In contrast, incomplete association was observed for markers from the region with the suggestive LRS. These results indicate that *d* is most likely located within the 14.2-cM region that includes markers *E16A12* and *E23C5*.

melanoid: Interval analysis revealed a single region of LG14 that was strongly associated with segregation of the *melanoid* mutant phenotype (*M1*, LRS 17.5, 95% C.I. = 32 cM) (Figure 3). As was the case with *white*, the founding and recurrent *A. mexicanum* parents that were used to generate the AxTg family were heterozygous for the *melanoid* mutant (M_{mex}/m_{mex}). The expressed sequence marker *E17A7* is closest to the maximum inflection point of the LRS profile for *melanoid*. Genotypic ratios for this locus are consistent with tight linkage to *melanoid*, given the same expectations described above for segregation of molecular markers and the *white* phenotype (Table 4).

Metamorphosis *vs.* paedomorphosis: Interval analysis revealed a single region of LG3 that was strongly associated with segregation of metamorphosis *vs.* paedomorphosis in the AxTg family (LRS 101.7, 95% C.I. = 9 cM) (Figure 4). The marker *ctg325* lies closest to the maximum inflection point of the LRS profile. This QTL is located near the middle of LG3 and corresponds to the previously described *met* QTL (VOSS and SHAFFER 1997; VOSS and SMITH 2005). A region of LG4 also showed a suggestive association with segregation of metamorphosis *vs.* paedomorphosis, although it is much weaker relative to *met*.

BLAST alignments to the human RefSeq database: Our BLASTx analysis of 570 EST/gene-based markers yielded alignments with multiple human protein-coding genes. In total, 390 presumptive protein-coding markers had best BLASTx alignments with 350 nonredundant human RefSeq proteins. Best BLASTx matches and corresponding bitscore and *E*-values are provided in supplementary Table S3 at <http://www.genetics.org/supplemental/>. Analyses of conserved synteny and

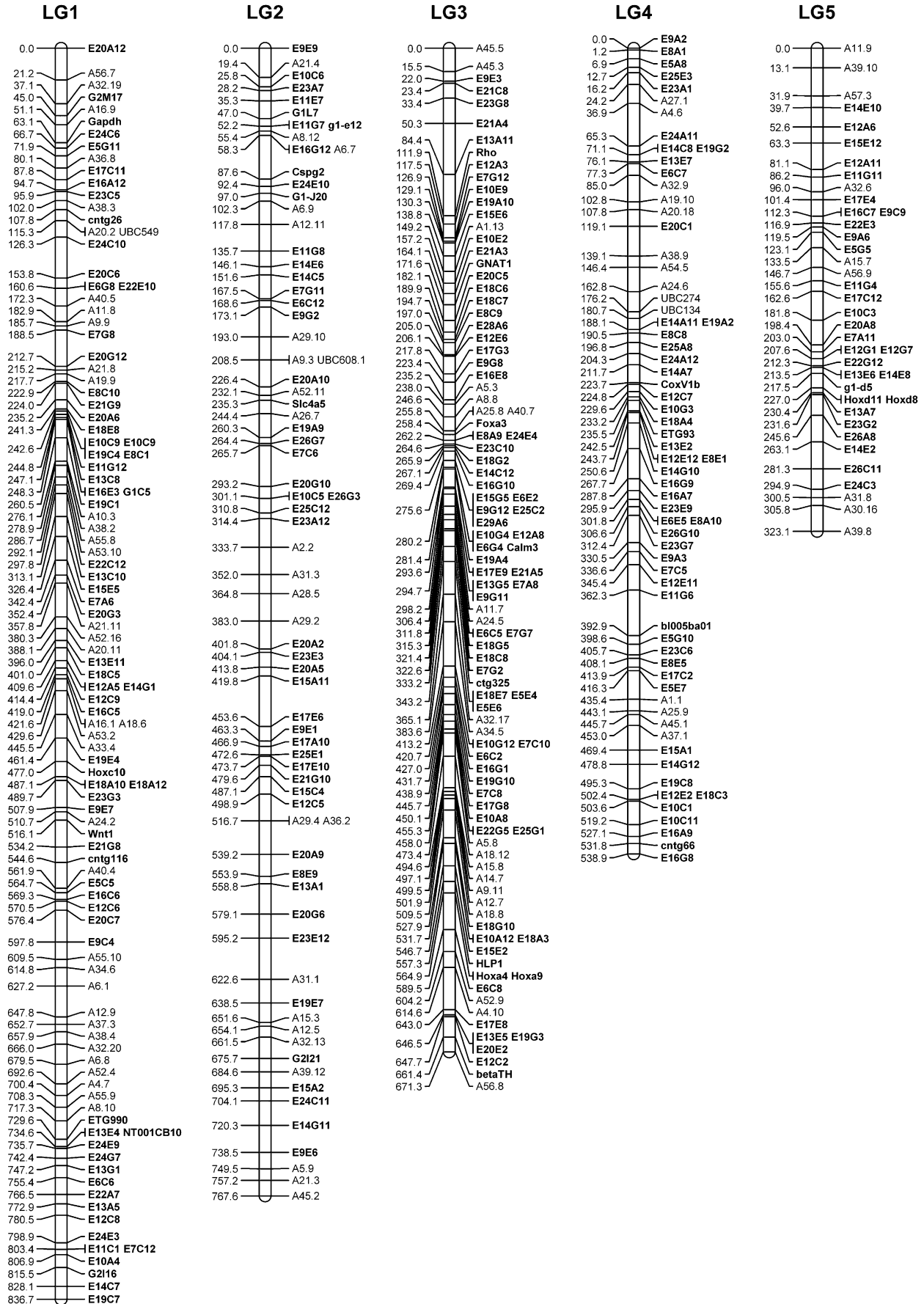


FIGURE 2.—The tiger salamander linkage map (LG1-14).

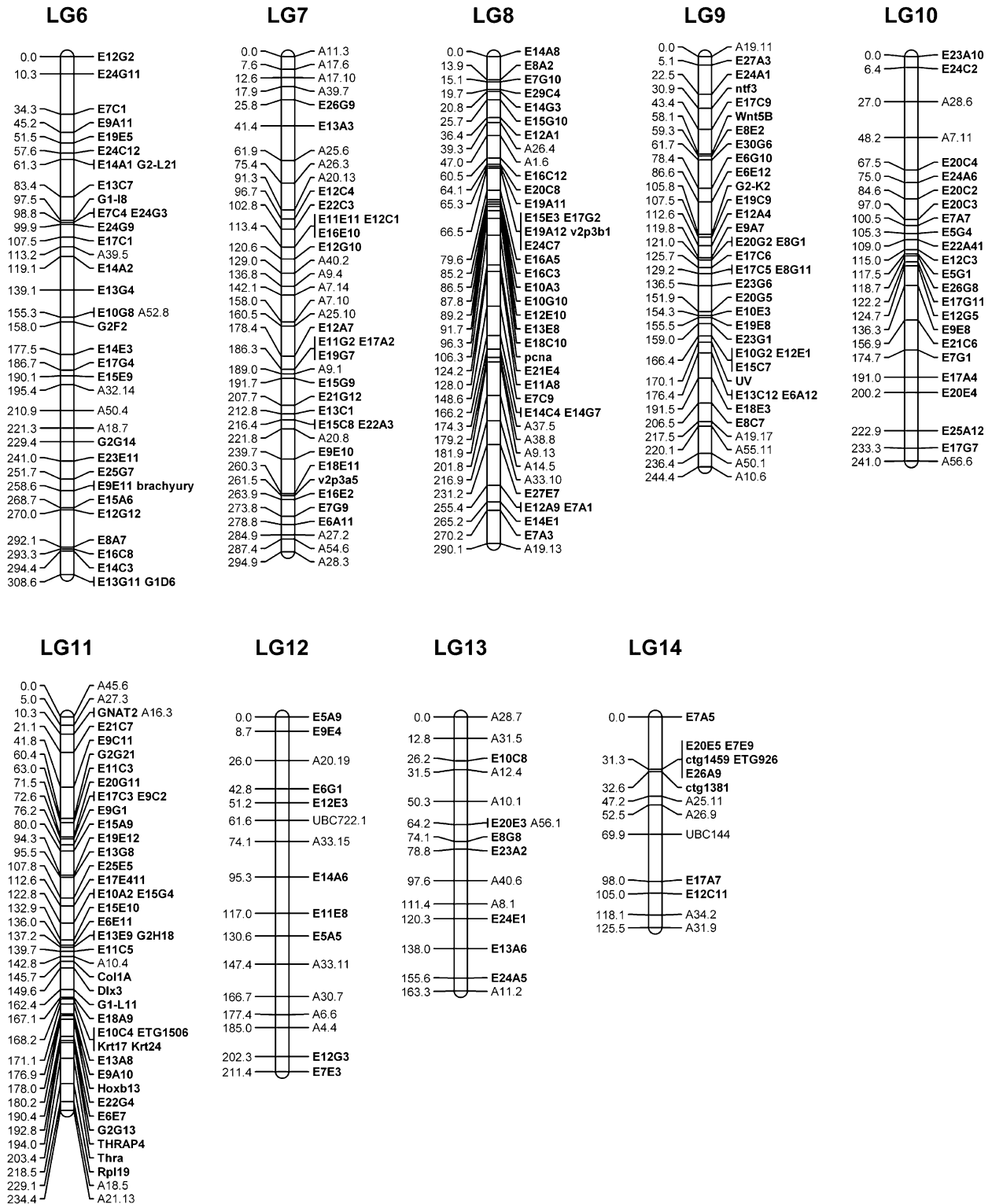


FIGURE 2.—Continued.

segmental homology between *Ambystoma* and other vertebrate species are presented elsewhere.

DISCUSSION

We have generated the first comprehensive linkage map for *Ambystoma* by mapping >1000 anonymous

markers and EST loci in an interspecific mapping panel. Fourteen large (>125–836 cM) and 35 small (0–75 cM) linkage groups were identified. Because the number of large linkage groups equaled the haploid chromosome number in *A. t. tigrinum* and *A. mexicanum* (PARAMENTER 1919; FANKHAUSER and HUMPHREY 1942), and because

TABLE 2
Distribution of markers on Ambystoma LG1–14

LG	EST based ^a	Anonymous markers ^a	All markers	cM	% map	Average intermarker distance
1	73 (70)	50 (37)	123 (107)	836.7	15.9	7.8
2	56 (51)	47 (24)	130 (75)	767.6	14.6	10.2
3	80 (78)	34 (21)	114 (99)	671.3	12.8	6.8
4	55 (54)	21 (14)	76 (68)	538.9	10.3	7.9
5	32 (30)	18 (9)	50 (39)	323.1	6.2	8.3
6	34 (34)	15 (5)	49 (39)	308.6	5.9	7.9
7	27 (25)	24 (17)	51 (42)	294.9	5.6	7.0
8	34 (34)	17 (8)	51 (42)	290.1	5.5	6.9
9	32 (31)	9 (5)	41 (36)	244.4	4.7	6.8
10	21 (21)	13 (3)	34 (24)	241.0	4.6	10.0
11	39 (38)	10 (6)	49 (44)	234.4	4.5	5.3
12	9 (9)	12 (7)	21 (16)	211.4	4.0	13.2
13	7 (7)	12 (8)	19 (15)	163.3	3.1	10.9
14	9 (9)	5 (5)	14 (14)	125.5	2.4	9.0
Total	508 (491)	287 (169)	795 (660)	5251.3	100.0	8.0
% mapped	87.4	54.7	71.9			

^aNumbers in parentheses represent the number of markers that were placed at precise positions within the map.

these linkage groups yielded a map size estimate that agrees with a theoretical and empirical (see below) estimate of total map size, we propose this set as a framework for the 14 chromosomes in the tiger salamander genome. It is unlikely that the collection of smaller linkage groups represent any additional chromosomes within the Ambystoma genome because the haploid chromosome number is indisputably 14 and microchromosomes are not known in this group.

Map coverage: The combined map distance of our 14 largest linkage groups (5251 cM) is consistent with previous studies that indicated a large genetic map for Ambystoma. By comparison, the combined map length of LG1 and LG2 is greater than the total map length of

the mouse genome! Marker-based estimates of genome size vary greatly for Ambystoma (*e.g.*, 2600–6276 cM in ARMSTRONG 1984 and 7291 cM in VOSS *et al.* 2001). This variation may be attributed to the large genome size of Ambystoma and the nonrobust nature of estimators; genotyping errors and missing data cause upward bias in size estimates and nonrandom distribution of markers with respect to recombinational distances causes downward bias (CHAKRAVARTI *et al.* 1991). We estimated genome size using linkage data from this study and the method of HULBERT *et al.* (1988). Analyses were performed separately for protein coding and anonymous marker classes and for the combined data set using several linkage thresholds (10, 15, 20, 25, and 30 cM; data not shown). Estimates of map size varied greatly depending on data set and linkage threshold: estimates based on protein-coding markers ranged from 3741 to 4320 cM (15 and 30 cM thresholds, respectively), estimates from anonymous markers ranged from 6925 to

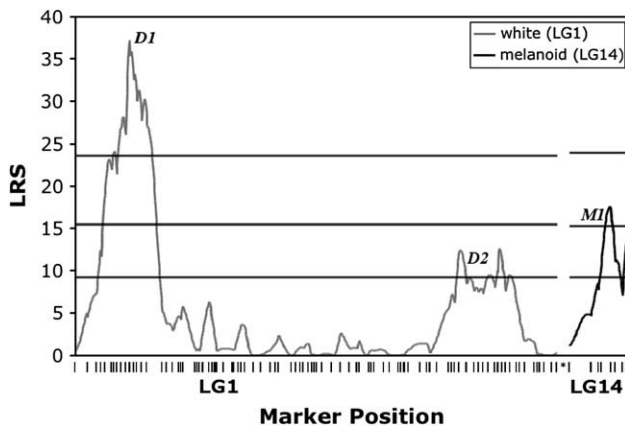


FIGURE 3.—LRS plot for association between segregation of pigment phenotypes and marker genotypes in LG1 and LG14. Horizontal lines represent LRS thresholds for suggestive (37th percentile), significant (95th percentile), and highly significant (99.9th percentile) associations (LANDER and KRUGLYAK 1995) estimated using MapMaker QTXb19.

TABLE 3
Segregation of markers associated with white

QTL	Genotype	Phenotype	
		white	+
<i>D1</i>	<i>E16A12^{Am}/E16A12^{Am}</i>	18	20
<i>D1</i>	<i>E16A12^{Am}/E16A12^{At}</i>	0	46
<i>D1</i>	<i>E23C5^{Am}/E23C5^{Am}</i>	18	18
<i>D1</i>	<i>E23C5^{Am}/E23C5^{At}</i>	0	43
<i>D2</i>	<i>A32.20^{Am}/A32.20^{Am}</i>	16	31
<i>D2</i>	<i>A32.20^{Am}/A32.20^{At}</i>	2	38

TABLE 4
Segregation of markers associated with *melanoid*

QTL	Genotype	Phenotype	
		<i>melanoid</i>	+
<i>MI</i>	<i>E24E9^{Am}/E24E9^{Am}</i>	10	30
<i>MI</i>	<i>E24E9^{Am}/E24E9^{At}</i>	6	41
<i>MI</i>	<i>E17A7^{Am}/E17A7^{Am}</i>	14	23
<i>MI</i>	<i>E17A7^{Am}/E17A7^{At}</i>	2	44

10,782 cM (25 and 10 cM thresholds, respectively), and estimates based on the entire data set ranged from 7624 to 8824 cM (25 and 10 cM thresholds, respectively). Presumably, higher intrinsic error rates of AFLP markers (*e.g.*, ISIDORE *et al.* 2003) (Figure 1, A and B) yield inflated estimates of map size in the anonymous and combined data sets.

Fortunately, a more direct and independent estimate of recombination frequency is available for *A. mexicanum*. CALLAN's (1966) counts of chiasmata in *A. mexicanum* oocyte nuclei convert to an estimated map size of 5650 cM. This estimate is only slightly higher than the sum of our 14 largest linkage groups (5251 cM). Several factors likely contribute to the relatively small difference between these two estimates, including incomplete coverage of the linkage map (especially near the telomeres), the degree to which the KOSAMBI (1944) mapping function models recombination in *Ambystoma*, variation in average recombination rate between the male F_1 's used in this study and the female *A. mexicanum* used by CALLAN (1966), and possibly small-scale differences in gene order between *A. t. tigrinum* and *A. mexicanum* (SYBENGA 1992; TRUE *et al.* 1996). Close agree-

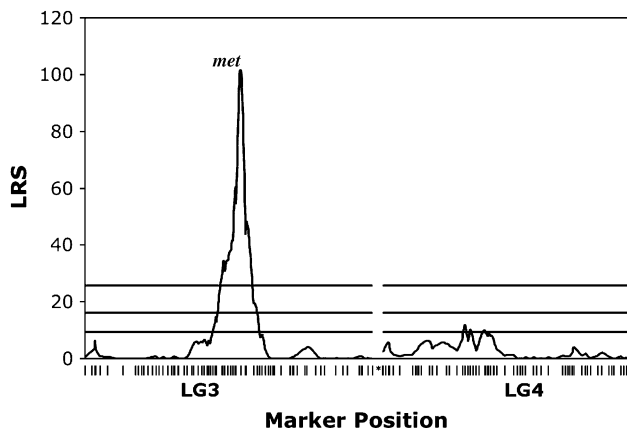


FIGURE 4.—LRS plot for association between segregation of metamorphosis *vs.* pedomorphosis and marker genotypes in LG3 and LG4. Horizontal lines represent LRS thresholds for suggestive (37th percentile), significant (95th percentile), and highly significant (99.9th percentile) associations (LANDER and KRUGLYAK 1995) estimated using MapMaker QTXb19.

ment between the CALLAN (1966)-derived estimate and our recombination-based estimates of genome size suggest that the 14 large linkage groups that we identified frame the majority of the *Ambystoma* genome.

Some of the smaller linkage groups may represent distal portions of chromosomes that are represented by larger linkage groups. Recombination rates are known to increase toward the ends of chromosomal arms in a wide array of organisms, including mammals (*e.g.*, JENSEN-SEMEN *et al.* 2004), chickens (INTERNATIONAL CHICKEN GENOME SEQUENCING CONSORTIUM 2005), and grasses (KING *et al.* 2002; ANDERSON *et al.* 2004). In agreement with this pattern, CALLAN (1966) reported a higher-than-average recombination rate between the nucleolar organizing region (NOR) and the adjacent telomere in *A. mexicanum*. Alternately, some of these linkage groups may consist completely or partly of markers with genotyping error rates that prevent assignment to larger linkage groups at the LOD 4.0 threshold. Presumably as more loci are mapped, linkage groups that represent distal regions will be integrated into the framework map and spurious linkage groups will be excluded from the map.

Size of the tiger salamander genetic map: The salamander genome is one of the largest genomes and our linkage map is the largest yet reported for any vertebrate. The tiger salamander genome is estimated to be 10–25 \times larger than other sequenced vertebrate genomes, yet the genetic map is only 1.5–5 \times larger (Table 1). Thus, in terms of genome size, the salamander linkage map appears to be \sim 5 \times smaller than expected. However, because physical and linkage distances do not scale linearly among organisms, variables in addition to physical size must be considered. Chromosome number contributes directly to the size of the genetic map because at least one chiasma must be formed per bivalent to ensure normal segregation of chromatids during meiosis in most species (EGEL 1995; ROEDER 1997; MOORE and ORR-WEAVER 1998), although achiasmate meiosis has evolved in several plant and invertebrate species (reviewed by JOHN 1990). Therefore, the minimum map size of any eukaryotic genome is 50 cM \times the haploid number of chromosomes. Furthermore, there is a strong correlation between chromosome arm number and genetic map size among mammals, suggesting that formation of at least one chiasma per chromosomal arm may be necessary in mammals (DURTILLEAUX 1986; PARDO-MANUEL DE VILLENA and SAPIENZA 2001). Map sizes for human, mouse, rat, chicken, and zebrafish are much closer to their theoretical obligatory minima, on the basis of chromosome arm number, than is the *Ambystoma* map (Table 1). Analyses that include multiple vertebrate taxa, especially those with large and intermediate genetic map lengths, are needed to fully elucidate the effect of chromosome arm number and other variables on genetic map size. However, it is apparent from the comparisons made here that linkage map size in *Ambystoma* is

influenced by factors in addition to chromosome arm number, the most likely factor being the large physical genome size of *Ambystoma*.

Refining the positional estimate of *white* and tentative assignment of LG1 to the chromosome harboring the NOR: The *white* phenotype has been a subject of several linkage analyses. Early tetrad mapping studies located *d* in the distal region of an unknown chromosome (LINDSLEY *et al.* 1955; ARMSTRONG 1984) and several studies have observed an association between segregation of *white* and segregation of NOR variants (reviewed by SINCLAIR *et al.* 1978). The NOR is located subterminally on one of the four largest chromosomes (PARAMENTER 1919; DEARING 1934; HASCHUKA and BRUNST 1965; CALLAN 1966; CUNY and MALACINSKI 1985). In our study we identified a single region of the genome that was significantly associated with *white*. The maximum inflection point of the LRS profile for association with *white* is located 95 cM from the end of the largest linkage group (LG1). CALLAN'S (1966) chiasmata counts place the NOR at ~44 cM from the end of a chromosomal arm. Localization of *white* to the distal portion of a large linkage group is consistent with previous studies that indicated linkage between *white* and the NOR. We therefore conclude that LG1 likely represents the NOR-containing chromosome, with marker *E20A12* located near the distal portion of the arm harboring the NOR.

Identification of the genomic interval containing *melanoid*: We have identified a single region within the smallest of our 14 linkage groups that shows strong association with segregation of the *melanoid* phenotype. ARMSTRONG'S (1984) tetrad analyses yielded an estimated distance of 59.1 cM between *melanoid* and its centromere. Assuming that LG14 corresponds to one of the smaller chromosomes, the maximum inflection point of the LRS profile for *melanoid* is consistent with the earlier gene-centromere mapping study. The size of LG14 relative to the rest of the genetic map appears to support the assignment of LG14 to the smallest chromosome. Precise chromosomal measurements have been made for *A. tigrinum* (PARAMENTER 1919) and *A. mexicanum* (CALLAN 1966); the proportion of the genome occupied by the smallest chromosome was estimated to be 2.65% for *A. tigrinum* and 2.4% for *A. mexicanum*. Our LG14 represents 2.4% of the current genetic map (LG1–14). Although we do not expect a linear relationship between genetic and physical distance, our results are consistent with *melanoid* being located on one of the smaller tiger salamander chromosomes.

The genetic basis of metamorphic failure in lab *A. mexicanum*: It has been known for some time that expression of paedomorphosis in laboratory *A. mexicanum* is largely determined by a single genetic factor (TOMPKINS 1978; VOSS 1995). A previous QTL analysis of the AxTg mapping panel using 234 AFLP markers identified a major-effect QTL (*met*) that is associated with

expression of paedomorphosis *vs.* metamorphosis (VOSS and SHAFFER 1997); *met* was later shown to affect metamorphic timing in crosses using wild-caught *A. mexicanum* (VOSS and SMITH 2005). Our QTL analysis using all of the newly mapped markers did not identify statistically significant factors in addition to *met*; however, a second region of the genome yielded a statistically suggestive result. The relatively small number of individuals in the AxTg panel does not provide sufficient power to identify small-effect QTL. This second genomic region will be tested using the much larger WILD2 mapping panel (VOSS and SMITH 2005) in future work.

EST markers and *Ambystoma* research: The collection of EST markers that constitute our linkage map are significant new resources for *Ambystoma* research. Because these markers correspond to polymorphic expressed sequences with known linkage relationships, they are especially informative as probes for developmental, populational, systematic, molecular, comparative, and functional studies (PUTTA *et al.* 2004). Using the PCR primer information provided in supplementary Table S1 at <http://www.genetics.org/supplemental/>, it will now be possible to develop probes for many protein-coding genes for *A. mexicanum* and *A. tigrinum*, as well as for other ambystomatid species (RILEY *et al.* 2003; FITZPATRICK and SHAFFER 2004; PUTTA *et al.* 2004). Primer sequences for protein-coding markers, their corresponding assembled and curated EST sequences, and BLAST alignments can also be obtained at the Salamander Genome Project website (<http://www.ambystoma.org>).

This work was supported by grants to S.R.V. from the National Science Foundation (IOB-0242833) and the National Center for Research Resources (NCRR: 5R24RR016344) at the National Institutes of Health (NIH). This research also utilized computing resources and facilities provided by the University of Kentucky subcontract from the NIH grant 2P20RR016481-04 from the NCRR.

LITERATURE CITED

- ANDERSON, L. K., N. SALAMEH, H. W. BASS, L. C. HARPER, W. Z. CANDE *et al.*, 2004 Integrating genetic linkage maps with pachytene chromosome structure in maize. *Genetics* **166**: 1923–1933.
- ARMSTRONG, J. B., 1984 Genetic mapping in the Mexican axolotl, *Ambystoma mexicanum*. *Can. J. Genet. Cytol.* **26**: 1–6.
- BACHVAROVA, R. F., T. MASI, M. DRUM, N. PARKER, K. MASON *et al.*, 2004 Gene expression in the axolotl germ line: *Axdazl*, *Axvh*, *Axoct-4*, and *Axkit*. *Dev. Dyn.* **231**: 871–880.
- BROWN, D. M., T. C. MATISE, G. KIOKE, J. S. SIMON, E. S. WINER *et al.*, 1998 An integrated linkage map of the laboratory rat. *Mamm. Genome* **9**: 521–530.
- CALLAN, H. G., 1966 Chromosomes and nucleoli of the axolotl, *Ambystoma mexicanum*. *J. Cell Sci.* **1**: 85–108.
- CHAKRAVARTI, A., L. K. LASHER and J. E. REEFER, 1991 A maximum-likelihood method for estimating genome length using genetic-linkage data. *Genetics* **128**: 175–182.
- CHEN, X., L. LEVINE and P-Y. KWOK, 1999 Fluorescence polarization in homogenous nucleic acid analysis. *Genome Res.* **9**: 492–498.
- CHICHILNISKY, E. J., and F. REIKE, 2005 Detection sensitivity and temporal resolution of visual signals near absolute threshold in the salamander retina. *J. Neurosci.* **25**: 310–330.

- CHRISTENSEN, R. N., M. WEINSTEIN and R. A. TASSAVA, 2002 Expression of fibroblast growth factors 4, 8, and 10 in limbs, flanks, and blastemas of *Ambystoma*. *Dev. Dyn.* **223**: 193–203.
- COLLINS, J. P., J. L. BRUNNER, J. K. JANCOVICH and D. M. SCHOCK, 2004 A model host-pathogen system for studying infectious disease dynamics in amphibians: tiger salamanders (*Ambystoma tigrinum*) and *Ambystoma tigrinum* virus. *Herpetol. J.* **14**: 195–200.
- CUNY, R., and G. M. MALACINSKI, 1985 Banding differences between tiger salamander and axolotl chromosomes. *Can. J. Genet. Cytol.* **27**: 510–514.
- DARVASI, A., and M. SOLLER, 1997 A simple method to calculate resolving power and confidence interval of QTL map location. *Behav. Genet.* **27**: 125–132.
- DEARING, W. H., 1934 The maternal continuity and individuality of the somatic chromosomes of *Ambystoma tigrinum*, with special reference to the nucleolus as a chromosomal component. *J. Morphol.* **56**: 157–179.
- DENZ, C. R., A. NARSHI, R. W. ZAJDEL and D. K. DUBE, 2004 Expression of a novel cardiac-specific tropomyosin isoform in humans. *Biochem. Biophys. Res. Commun.* **320**: 1291–1297.
- DUMERIL, A. H. A., 1870 Quatrième notice sur la menagerie des reptiles du Muséum d'Historie Naturelle. *Nouveau Archives du Muséum d'Historie Naturelle, Paris, Vol. 5*, pp. 47–60.
- DURTILLEAUX, B., 1986 Le rôle des chromosomes dans l'évolution: une nouvelle interprétation. *Ann. Genet.* **29**: 69–75.
- EGEL, E. R., 1995 The synaptonemal complex and the distribution of meiotic recombination events. *Trends Genet.* **11**: 206–208.
- ERICSSON, R., R. CERNY, P. FALCK and L. OLSSON, 2004 Role of cranial neural crest cells in visceral arch muscle positioning and morphogenesis in the Mexican axolotl, *Ambystoma mexicanum*. *Dev. Dyn.* **231**: 237–247.
- FANKHAUSER, G., and R. R. HUMPHREY, 1942 Induction of triploidy and haploidy in axolotl eggs by cold treatment. *Biol. Bull.* **83**: 367–374.
- FITZPATRICK, B. M., and H. B. SHAFFER, 2004 Environment-dependent admixture dynamics in a tiger salamander hybrid zone. *Evolution* **58**: 1282–1293.
- GARDINER, A. F., and W. E. JACK, 2002 Acyclic and dideoxy terminator preferences denote divergent sugar by archaeon detection. *BioTechniques* **31**: 560–570.
- GORNUNG, E., I. GABRIELLI, S. CATAUDELLA and L. SOLA, 1997 CMA(3)-banding pattern and fluorescence in situ hybridization with 18s rRNA genes in zebrafish chromosomes. *Chromosome Res.* **5**: 40–46.
- GOULD, S. J., 1977 *Ontogeny and Phylogeny*. Belknap Press, Cambridge, MA.
- GROENEN, M. A. M., H. H. CHENG, N. BUMSTEAD, B. F. BENKEL, W. E. BRILES *et al.*, 2000 A consensus linkage map of the chicken genome. *Genome Res.* **10**: 137–147.
- HABERMAN, E. T., A-G. BEBIN, S. HERKLOTZ, M. VOLKMER, K. ECKELT *et al.*, 2004 An *Ambystoma mexicanum* EST sequencing project: analysis of 17,352 expressed sequence tags from embryonic and regenerating blastema cDNA libraries. *Genome Biol.* **5**: R67.
- HÄCKER, V., 1907 Über mendelschen vererbung bei axolothn. *Zoologischer Anzeiger* **31**: 99–102.
- HALEY, C. S., and S. A. KNOTT, 1992 A simple regression method for mapping quantitative trait loci in line crosses using flanking markers. *Heredity* **69**: 315–324.
- HASCHUKA, T. S., and V. V. BRUNST, 1965 Sexual dimorphism in the nuclear autosome of the axolotl (*Sirenodon mexicanum*). *Hereditas* **52**: 345–356.
- HOFFMAN, E. A., and D. W. PFENNIG, 1999 Proximate causes of cannibalistic polyphenism in larval tiger salamanders. *Ecology* **80**: 1076–1080.
- HSU, T. M., X. CHEN, S. DUAN, R. D. MILLER and P-Y. KWOK, 2001 Universal SNP genotyping assay with fluorescence polarization detection. *Nucleic Acids Res.* **30**: 605–613.
- HULBERT, S., T. W. ILOTT, E. J. LEGG, S. E. LINCLON, E. S. LANDER *et al.*, 1988 Genetic analysis of the fungus, *Bremia lactucae*, using restriction fragment length polymorphisms. *Genetics* **120**: 947–958.
- HUMPHREY, R. R., and J. T. BAGNARA, 1967 A color variant in the Mexican axolotl. *J. Hered.* **58**: 251–256.
- INTERNATIONAL CHICKEN GENOME SEQUENCING CONSORTIUM, 2005 Sequence and comparative analysis of the chicken genome provide unique perspectives on vertebrate evolution. *Nature* **432**: 695–716.
- INTERNATIONAL HUMAN GENOME SEQUENCING CONSORTIUM, 2001 Initial sequencing and analysis of the human genome. *Nature* **409**: 860–921.
- IRSCHICK, D. J., and H. B. SHAFFER, 1997 The polytypic species revisited: morphological differentiation among tiger salamanders (*Ambystoma tigrinum*) (Amphibia: Caudata). *Herpetologica* **53**: 30–49.
- ISIDORE, E., H. VAN OS, S. ANDRZEJEWSKI, J. BAKKER, I. BARRENA *et al.*, 2003 Toward a marker dense linkage map of the potato genome: lesions from linkage group I. *Genetics* **165**: 2107–2116.
- JENSEN-SEMEN, M. I., T. S. FURLEY, B. A. PAYSEUR, Y. LU, K. M. ROSKIN *et al.*, 2004 Comparative recombination rates in the rat, mouse, and human genomes. *Genome Res.* **14**: 528–538.
- JOHN, B., 1990 *Meiosis*. Cambridge University Press, Cambridge, UK.
- KELLY, P. D., F. CHU, I. G. WOODS, P. NGO-HAZELETT, T. CARDOZO *et al.*, 2000 Genetic linkage mapping of zebrafish genes and ESTs. *Genome Res.* **10**: 558–567.
- KING, J., L. A. ROBERTS, M. J. KEARSEY, H. M. THOMAS, R. N. JONES *et al.*, 2002 A demonstration of a 1:1 correspondence between chiasmata frequency and recombination using a *Lolium perenne*/*Festuca pratensis* substitution. *Genetics* **161**: 307–314.
- KONG, A., D. F. GUBDJARTSSON, J. SAINZ, G. M. JONSDOTTIR, S. A. GUDJONSSON *et al.*, 2002 A high resolution recombination map of the human genome. *Nat. Genet.* **31**: 241–247.
- KOSAMBI, D. D., 1944 The estimation of map distances from recombination values. *Ann. Eugen.* **12**: 172–175.
- LANDER, E., and L. KRUGLYAK, 1995 Genetic dissection of complex traits: guidelines for interpreting and reporting linkage results. *Nat. Genet.* **11**: 241–247.
- LICHT, L. E., and L. A. LOWCOCK, 1991 Genome size and metabolic rate in salamanders. *Comp. Biochem. Physiol. B, Biochem. Mol. Biol.* **100**: 83–92.
- LINDSLEY, D. L., G. FANKHAUSER and R. R. HUMPHREY, 1955 Mapping centromeres in the axolotl. *Genetics* **41**: 58–64.
- MALACINSKI, G. M., 1989 Developmental genetics, pp. 102–109 in *Developmental Biology of the Axolotl*, edited by J. B. ARMSTRONG and G. M. MALACINSKI. Oxford University Press, New York.
- MARCHAND, J. E., X. H. YANG, D. CHIKARAISHI, J. KRIEGER, H. BREER *et al.*, 2004 Olfactory receptor gene expression in tiger salamander olfactory epithelium. *J. Comp. Neurol.* **474**: 453–467.
- MARTINEZ, O., and R. N. CURNOW, 1992 Estimating the locations and the sizes of the effects of quantitative trait loci using flanking markers. *Theor. Appl. Genet.* **85**: 480–488.
- MASABANDA, J. S., D. W. BURT, C. M. O'BRIEN, A. VIGNAL, V. FILLON *et al.*, 2004 Molecular cytogenetic definition of the chicken genome: the first complete avian karyotype. *Genetics* **166**: 1367–1373.
- MEER, J. M., R. H. CUDMORE, JR. and K. F. MANLY, 2004 Map-Manager QTX (<http://www.mapmanager.org/mmQTX.html>).
- MOORE, D. P., and T. L. ORR-WEAVER, 1998 Chromosome segregation during meiosis: building an unambivalent bivalent. *Top. Dev. Biol.* **37**: 263–299.
- MOUSE GENOME SEQUENCING CONSORTIUM, 2002 Initial sequencing and comparative analysis of the mouse genome. *Nature* **420**: 520–562.
- PARAMENTER, C. L., 1919 Chromosome number and pairs in somatic mitoses of *Ambystoma tigrinum*. *J. Morphol.* **33**: 169–249.
- PARDO-MANUEL DE VILLENA, F., and C. SAPIENZA, 2001 Recombination is proportional to the number of chromosome arms in mammals. *Mamm. Genome* **12**: 318–322.
- PARICHY, D. M., 1996 Pigment patterns of larval salamanders (Ambystomatidae, Salamandridae): the role of the lateral line sensory system and the evolution of pattern-forming mechanisms. *Dev. Biol.* **175**: 265–282.
- PARICHY, D. M., 1998 Experimental analysis of character coupling across a complex life cycle: pigment pattern metamorphosis in the tiger salamander, *Ambystoma tigrinum tigrinum*. *J. Morphol.* **237**: 53–67.
- PARICHY, D. M., M. STIGSON and S. R. VOSS, 1999 Genetic analysis of *steel* and the PG-M/versican-encoding gene *AxPG* as candidates for the white (*d*) pigment mutant in the salamander *Ambystoma mexicanum*. *Dev. Genes Evol.* **209**: 349–356.

- PARK, D., J. M. MCGUIRE, A. L. MAJCHRZAK, J. M. ZIOBRO and H. L. EISTHEN, 2004 Discrimination of conspecific sex and reproductive condition using chemical cues in axolotls (*Ambystoma mexicanum*). *J. Comp. Physiol. A* **190**: 415–427.
- POWERS, J. H., 1907 Morphological variation and its causes in *Ambystoma tigrinum*. Studies of the University of Nebraska **7**: 197–274.
- PUTTA, S., J. J. SMITH, J. WALKER, M. RONDET, D. W. WEISROCK *et al.*, 2004 From biomedicine to natural history research: EST resources for ambystomatid salamanders. *BMC Genomics* **5**: 54.
- RAT GENOME SEQUENCING PROJECT CONSORTIUM, 2004 Genome sequence of the brown Norway rat yields insights into mammalian evolution. *Nature* **428**: 493–521.
- REESE, R. W., 1969 The taxonomy and ecology of the tiger salamander *Ambystoma tigrinum* of Colorado. Ph.D. Thesis, University of Colorado, Boulder, CO.
- RILEY, S. P. D., H. B. SHAFFER, S. R. VOSS and B. M. FITZPATRICK, 2003 Hybridization between a rare, native tiger salamander (*Ambystoma californiense*) and its introduced congener. *Ecol. Appl.* **13**: 1263–1275.
- ROEDER, G. S., 1997 Meiotic chromosomes: it takes two to tango. *Genes Dev.* **11**: 2600–2621.
- ROSE, F. L., and D. ARMENTROUT, 1976 Adaptive strategies of *Ambystoma tigrinum* Green inhabiting the Llano Estacado of West Texas. *J. Anim. Ecol.* **45**: 713–739.
- SCHNAPP, E., and E. M. TANAKA, 2005 Quantitative evaluation of morpholino-mediated protein knockdown of *GFP*, *MSX1*, and *PAX7* during tail regeneration in *Ambystoma mexicanum*. *Dev. Dyn.* **232**: 162–170.
- SHAFFER, H. B., 1984 Evolution in a paedomorphic lineage. II. Allometry and form in the Mexican ambystomatid salamanders. *Evolution* **38**: 1207–1218.
- SHAFFER, H. B., and M. L. MCKNIGHT, 1996 The polytypic species revisited: genetic differentiation and molecular phylogenetics of the tiger salamander species *Ambystoma tigrinum* (Amphibia: Caudata) species complex. *Evolution* **50**: 417–433.
- SHAFFER, H. B., and S. R. VOSS, 1996 What insights into the developmental traits of urodeles does the study of interspecific hybrids provide? *Int. J. Dev. Biol.* **40**: 885–893.
- SINCLAIR, J. H., C. R. CARROL and G. M. MALACINSKI, 1978 Composition and behavior of the nucleolar organizer of the nucleolar variant of axolotls: review and comparison to other systems. *Am. Zool.* **18**: 225–236.
- SMITH, H. M., 1989 Discovery of the axolotl and its early history in biological research, pp. 1–12 in *Developmental Biology of the Axolotl*, edited by J. B. ARMSTRONG and G. M. MALACINSKI. Oxford University Press, New York.
- STEEN, R. G., A. E. KITWECK-BLACK, C. GLENN, J. GULLINGS-HANDLEY, W. VAN ETTEN *et al.*, 1999 A high density integrated genetic linkage and radiation hybrid map of the laboratory rat. *Genome Res.* **9**: AP1–AP8.
- STURTEVANT, A. H., 1913 The linear arrangement of six sex-linked factors in *Drosophila*, as shown by their mode of association. *J. Exp. Zool.* **14**: 43–59.
- SYBENGA, J., 1992 *Cytogenetics in Plant Breeding: Monographs on Theoretical and Applied Genetics*. Springer-Verlag, Berlin.
- THORESON, W. B., K. RABL, E. TOWNES-ANDERSON and R. HEILELBERGER, 2004 A highly Ca²⁺-sensitive pool of vesicles contributes to linearity at the rod photoreceptor ribbon synapse. *Neuron* **42**: 595–605.
- TOMPkins, R., 1978 Genetic control of axolotl metamorphosis. *Am. Zool.* **18**: 313–319.
- TRUE, J. R., B. S. WEIR and C. C. LAURIE, 1996 A genome-wide survey of hybrid incompatibility factors by the introgression of marked segments of *Drosophila mauritiana* chromosomes into *Drosophila simulans*. *Genetics* **142**: 819–837.
- VOORIPS, R. E., 2002 MapChart (<http://www.plant.wageningenur.nl/products/mapping/MapChart>).
- VOSS, S. R., 1995 Genetic basis of paedomorphosis in the axolotl *Ambystoma mexicanum*: a test of the single gene hypothesis. *J. Hered.* **86**: 441–447.
- VOSS, S. R., and H. B. SHAFFER, 1997 Adaptive evolution via a major gene effect: paedomorphosis in the Mexican axolotl. *Proc. Natl. Acad. Sci. USA* **94**: 14185–14189.
- VOSS, S. R., and J. J. SMITH, 2005 Evolution of salamander life cycles: a major effect QTL contributes to discrete and continuous variation for metamorphic timing. *Genetics* **170**: 275–281.
- VOSS, S. R., J. J. SMITH, D. M. GARDINER and D. M. PARICHY, 2001 Conserved vertebrate chromosomal segments in the large salamander genome. *Genetics* **158**: 735–746.
- ZENG, Z.-B., 1993 Theoretical basis for separation of multiple linked gene effects in mapping quantitative trait loci. *Proc. Natl. Acad. Sci. USA* **90**: 10972–10976.
- ZENG, Z.-B., 1994 Precision mapping of quantitative trait loci. *Genetics* **136**: 1457–1468.
- ZHANG, C., F. MENG, X. P. HUANG, R. ZAJDEL, S. L. LEMANSKI *et al.*, 2004 Down regulation of N1 gene expression inhibits the initial heart beating and heart development in axolotls. *Tissue Cell* **36**: 71–81.

Communicating editor: A. LONG